

# Pleiotropic Effects of ATP·Mg<sup>2+</sup> Binding in the Catalytic Cycle of Ubiquitin-activating Enzyme\*

Received for publication, December 21, 2005, and in revised form, March 13, 2006. Published, JBC Papers in Press, April 4, 2006, DOI 10.1074/jbc.M513562200

Zeynep Tokgöz<sup>†1</sup>, Richard N. Bohnsack<sup>‡</sup>, and Arthur L. Haas<sup>§2</sup>

From the <sup>†</sup>Department of Biochemistry, Medical College of Wisconsin, Milwaukee, Wisconsin 53226 and the <sup>§</sup>Department of Biochemistry and Molecular Biology and the Stanley S. Scott Cancer Center, Louisiana State University Health Sciences Center, New Orleans, Louisiana 70112

Conjugation of ubiquitin and other Class 1 ubiquitin-like polypeptides to specific protein targets serves diverse regulatory functions in eukaryotes. The obligatory first step of conjugation requires ATP-coupled activation of the ubiquitin-like protein by members of a superfamily of evolutionarily related enzymes. Kinetic and equilibrium studies of the human ubiquitin-activating enzyme (HsUba1a) reveal that mutations within the ATP·Mg<sup>2+</sup> binding site have remarkably pleiotropic effects on the catalytic phenotype of the enzyme. Mutation of Asp<sup>576</sup> or Lys<sup>528</sup> results in dramatically impaired binding affinities for ATP·Mg<sup>2+</sup>, a shift from ordered to random addition in co-substrate binding, and a significantly reduced rate of ternary complex formation that shifts the rate-limiting step to ubiquitin adenylate formation. Mutations at neither position affect the affinity of HsUbc2b binding; however, differences in *k*<sub>cat</sub> values determined from ternary complex formation *versus* HsUbc2b transthiolation suggest that binding of the E2 enhances the rate of bound ubiquitin adenylate formation. These results confirm that Asp<sup>576</sup> and Lys<sup>528</sup> are important for ATP·Mg<sup>2+</sup> binding but are essential catalytic groups for ubiquitin adenylate transition state stabilization. The latter mechanistic effect explicates the observed loss-of-function phenotype associated with mutation of residues paralogous to Asp<sup>576</sup> within the activating enzymes for other ubiquitin-like proteins.

The conjugation of ubiquitin and ubiquitin-like polypeptides to specific protein targets represents a fundamental and highly conserved strategy of eukaryotic cell regulation, reviewed most recently in Refs. 1–3. Post-translational modification by these polypeptides requires formation of isopeptide bonds through distinct yet evolutionarily related enzyme pathways that share a common mechanism in which the half-reactions of activation and ligation are catalyzed by distinct enzymes (1, 4). The ubiquitin-activating enzyme (Uba1)<sup>3</sup> catalyzes the first step in the conjugation of ubiquitin to protein targets and serves as the archetype for paralogous steps in the activation of other Class 1 ubiquitin-like proteins, including Sumo (5, 6), Nedd8 (7, 8), ISG15 (9), Hub1 (10), FAT10 (11, 12), and Apg12 (13) among others, reviewed in Refs. 14 and

15. The reaction follows a mechanism in which binding of ATP·Mg<sup>2+</sup> precedes binding of ubiquitin and the subsequent formation of a tightly bound ubiquitin adenylate intermediate (16, 17), a mixed acyl-phosphate anhydride between the carboxyl-terminal glycine of ubiquitin and AMP derived from the  $\alpha/\beta$  cleavage of ATP (18). Ubiquitin adenylate is the immediate precursor for formation of a covalent Uba1-ubiquitin thiolester intermediate at a conserved active site cysteine (Cys<sup>632</sup>, HsUba1a numbering), which is followed by a second round of ubiquitin adenylate formation to yield a Uba1 ternary complex composed of stoichiometric amounts of ubiquitin adenylate and ubiquitin thiolester (16). The Uba1-ubiquitin thiolester is the proximal donor of activated ubiquitin in formation of E2/Ubc-ubiquitin thiolesters required in all ubiquitin conjugation reactions (16, 19).

Because these conjugation pathways are universally conserved among eukaryotes<sup>4</sup> but are absent from prokaryotes and Archaea (4), the evolutionary origins of ubiquitin ligation had remained an enduring paradox. However, recent studies reveal remarkable sequence similarities between the highly conserved E1<sup>5</sup> paralogs and the MoeB subunit of *Escherichia coli* molybdopterin synthase, a multimeric enzyme complex that is involved in the evolutionarily conserved molybdenum cofactor (Moco) biosynthetic pathway found in both prokaryotes and eukaryotes (20, 21). The mechanism for molybdenum cofactor synthesis requires the MoeB-catalyzed activation of the carboxyl terminus of the 8757-Da MoaD subunit by formation of a tightly bound MoaD adenylate intermediate (20), a reaction mechanistically analogous to the Uba1-catalyzed activation of ubiquitin (16, 17). The 1.7-Å crystal structure of the MoeB-ATP-MoaD ternary complex of molybdopterin synthase provided early insights into the mechanism for the activation of MoaD, which shares a common  $\beta$ -grasp fold and a carboxyl-terminal Gly-Gly motif with ubiquitin (21). Subsequent high resolution structures for free and substrate-bound forms of the human paralogs of the AppBp1-Uba3 Nedd8-activating enzyme (22, 23) and the Sae1-Sae2 Sumo-activating enzyme (24), in addition to parallel chemistries for carboxyl group activation of their cognate polypeptide substrates, reveal a common active site fold for this E1 superfamily and suggest that MoeB and MoaD are the previously unidentified evolutionary precursors for Uba1 and ubiquitin, respectively.

The active site residues of MoeB that interact directly with ATP are highly conserved among Uba1 orthologs and E1 paralogs for Sumo, Nedd8, and ISG15 (21, 22). Extant structures for this superfamily identify an aspartate residue that either directly (24) or inferentially (21, 23) interacts with Mg<sup>2+</sup> chelated to bound ATP. The importance of this residue is suggested by its absolute conservation among MoeB and E1

\* This work was supported by United States Public Health Service Grant GM34009 (to A. L. H.). The costs of publication of this article were defrayed in part by the payment of page charges. This article must therefore be hereby marked "advertisement" in accordance with 18 U.S.C. Section 1734 solely to indicate this fact.

<sup>1</sup> Present address: St. Jude Children's Research Hospital, Dept. of Structural Biology, 332 N. Lauderdale, Memphis, TN 38105-2794.

<sup>2</sup> To whom correspondence should be addressed: Dept. of Biochemistry and Molecular Biology, LSU Health Sciences Center, 1901 Perdido St., New Orleans, LA 70112. Tel.: 504-568-3004; Fax: 504-568-3370; E-mail: ahaas@lsuhsc.edu.

<sup>3</sup> The abbreviations used are: Uba1, ubiquitin-activating enzyme; DTT, dithiothreitol; E1, generic term for activating enzymes of Class 1 ubiquitin-like proteins; E2/Ubc, ubiquitin carrier protein or ubiquitin-conjugating enzyme; HsUba1a, human nuclear form of ubiquitin-activating enzyme; HsUbc2b, "b" isoform of the human/rabbit ortholog of *Saccharomyces cerevisiae* Rad6/Ubc2 (also termed E2<sub>14kb</sub>); GST, glutathione S-transferase; Ub, ubiquitin.

<sup>4</sup> The single exception is the ubiquitin-like protein ISG15, which is found only among vertebrates and thus represents an evolutionarily recent diverged pathway apparently required for unique functions (45, 46).

<sup>5</sup> We shall use E1 generically to refer to the paralogous activating enzymes for Class 1 ubiquitin-like proteins.

## ATP-Mg<sup>2+</sup> Binding to the Ubiquitin-activating Enzyme

paralogs as well as the dramatic effects of point mutagenesis. Mutation of Asp<sup>130</sup> to alanine abrogates MoeB activity in *E. coli* (21), whereas mutations of the paralogous Asp<sup>146</sup> of Uba3 or Asp<sup>117</sup> of Sae2 significantly ablate Nedd8 and Sumo activation by human AppBp1-Uba3 or Sae1-Sae2 heterodimers, respectively (22, 24). However, loss-of-function mutations are rarely informative without additional studies, since the phenotype cannot be unambiguously interpreted. Thus, whereas the loss-of-function mutations that arise from nonconservative changes in Asp<sup>130</sup> and its paralogous residues are consistent with their predicted roles in ATP-Mg<sup>2+</sup> binding, collateral mechanistic and/or structural effects cannot be precluded.

To understand more completely the mechanistic contribution of the aspartate residue in the catalytic cycle of human ubiquitin-activating enzyme and its paralogs, we have introduced a series of point mutations at Asp<sup>576</sup> of human Uba1a that corresponds to Asp<sup>130</sup> of *E. coli* MoeB, Asp<sup>146</sup> of human Uba3, and Asp<sup>117</sup> of human Sae2. Kinetic analyses confirm a role for Asp<sup>576</sup> in ATP-Mg<sup>2+</sup> binding. However, the point mutants also exhibit pleiotropic effects on the mechanism of ubiquitin activation, including transition state stabilization and order of substrate binding, that reveal a more complex role not anticipated in earlier studies. Such insights identify Asp<sup>576</sup> and its paralogs as critical catalytic residues in the reaction cycle of this enzyme family.

### MATERIALS AND METHODS

Bovine ubiquitin, creatine phosphokinase, and yeast inorganic pyrophosphatase were purchased from Sigma. The ubiquitin was further purified to apparent homogeneity and then radioiodinated by the chloramine-T procedure (25, 26). Carrier-free Na<sup>125</sup>I, [2,8-<sup>3</sup>H]ATP, and Na<sub>4</sub><sup>32</sup>PP<sub>i</sub> were purchased from PerkinElmer Life Sciences. Recombinant human HsUbc2b and the active site mutant HsUbc2bC88A were those described previously (27).

**Generation of GST-HsUba1a Point Mutants**—A pGEX3X-E1 construct encoding the nuclear form of the human ubiquitin-activating enzyme (HsUba1a), generously provided by Dr. Alan L. Schwartz (Washington University School of Medicine), was used for the expression of wild type and mutant HsUba1a enzymes. The D576A, D576E, and D576N point mutants of HsUba1a were generated by the PCR overlap extension method of Ho *et al.* (28) using pGEX3X-E1 as a template. Point mutations were introduced using internal primers containing the desired mutation and external primers flanking the region of the gene bound by XhoI and Eco72RI restriction sites. Following PCR amplification of the corresponding single site mutations, inserts were subcloned into the pGEM-T vector. The subcloned insert was digested with XhoI/Eco72RI restriction enzymes, agarose gel-purified, and then ligated into a similarly restricted pGEX3X vector. Mutations were confirmed by sequencing the complete XhoI/Eco72RI inserts on an Applied Biosystems ABI Prism 3100 DNA sequencer.

**Expression and Purification of GST-HsUba1a Wild Type and Mutant Proteins**—*E. coli* BL21 (DE3) cells were transformed with pGEX3X encoding either wild type or mutant forms of ubiquitin-activating enzyme. Single colonies harboring the appropriate vector (pGEX3X-wtE1, pGEX3X-E1D576A, pGEX3X-E1D576N, or pGEX3X-E1D576E) were inoculated into 50 ml of LB medium containing 100 μg/ml ampicillin and then grown to stationary phase at 30 °C. This culture was used to inoculate 500 ml of LB-ampicillin medium at a final dilution of 1:25 and then grown to an A<sub>600</sub> of 0.6 at 30 °C with constant shaking. Protein expression was induced by the addition of isopropyl 1-thio-β-D-galactopyranoside to a final concentration of 0.3 mM, after which the culture was allowed to grow an additional 2 h. The cells were harvested by centrifugation and then resuspended in ice-cold 50 mM Tris-HCl (pH

7.5), 2 mM EDTA, and 1 mM DTT. All subsequent steps were conducted at 4 °C. The resuspended cells were lysed by a French press, and the cell debris was removed by centrifugation at 100,000 × *g* for 30 min. The resulting supernatant was loaded onto a glutathione-agarose affinity column (Sigma) equilibrated with 50 mM Tris-HCl (pH 7.5) and 1 mM DTT. The GST wild type and mutant human Uba1a fusions were eluted with 20 mM reduced glutathione in 50 mM Tris-HCl (pH 7.5) and 1 mM DTT and then dialyzed overnight against 50 mM Tris-HCl (pH 7.5) containing 1 mM DTT. The purified proteins were analyzed by 7.5% SDS-PAGE, followed by Western blotting and subsequent visualization using anti-GST antibodies and ECL detection. Protein concentrations for full-length wild type and mutant HsUba1a enzymes were normalized to GST content using quantitative Western blotting.

**Enzyme Assays**—Concentrations of active wild type and mutant GST-HsUba1a enzymes were determined by the stoichiometric formation of <sup>125</sup>I-ubiquitin thiolester from free radioiodinated ubiquitin (~5000 cpm/pmol) in end point assays, followed by nonreducing SDS-PAGE resolution and γ counting of associated <sup>125</sup>I radioactivity in excised bands (16). Enzyme-bound ubiquitin [<sup>3</sup>H]adenylate formation was determined using [2,8-<sup>3</sup>H]ATP (3.6 × 10<sup>4</sup> cpm/pmol) and measured by trichloroacetic acid-precipitable radioactivity (16). Initial rates of ATP/<sup>32</sup>PP<sub>i</sub> exchange were measured at the indicated concentrations of ATP, ubiquitin, <sup>32</sup>PP<sub>i</sub>, and either GST-HsUba1a or the corresponding Asp<sup>576</sup> or Lys<sup>528</sup> mutants (17). Initial rates of HsUbc2b-<sup>125</sup>I-ubiquitin thiolester formation were measured by nonreducing SDS-PAGE in HsUba1a-catalyzed transthiolation assays at the indicated concentrations of ATP, <sup>125</sup>I-ubiquitin, and recombinant HsUbc2b (27). For Asp<sup>576</sup> mutants of GST-HsUba1a, initial rates of HsUba1a-<sup>125</sup>I-ubiquitin thiolester formation were measured directly by modification of the E2 transthiolation assay (27).

### RESULTS

**Only Full-length GST-HsUba1a Is Active**—Expression of wild type or mutant GST-HsUba1a consistently yielded a mixture of full-length protein (*M<sub>r</sub>* 136,000) and a ladder of GST-linked fusion protein fragments when detected by Coomassie staining after SDS-PAGE resolution (not shown) or by Western blot using anti-GST antibodies (Fig. 1). Although the protein expression yielded a mixture of full-length and partially degraded fusion protein, only full-length GST-HsUba1a was active in forming the corresponding <sup>125</sup>I-ubiquitin thiolester (Fig. 1). The amount of GST-HsUba1a-<sup>125</sup>I-ubiquitin thiolester calculated from the specific radioactivity of the labeled polypeptide agreed well with that predicted from the protein content of the full-length GST-HsUba1a fusion protein estimated by Coomassie staining and comparison with a known amount of bovine serum albumin (not shown).

Thus, a carboxyl-terminal segment of 20 kDa, representing ~170 amino acids, is essential for the activity of HsUba1. The cleavage point for this fragment lies between the predicted carboxyl-terminal β-grasp domain common to all members of the E1 superfamily (22) and the thiolester active site located at Cys<sup>632</sup>. However, other studies showed that truncation of the 118-residue predicted β-grasp domain from the carboxyl terminus of HsUba1a had no effect on the stoichiometry of the resulting mutant<sup>6</sup>; therefore, the critical region must lie within a 52-amino acid segment between residues 888 and 940 of the intact protein. Crystal structures for MoeB, AppBp1-Uba3, and Sae1-Sae2 show that the paralogous regions for the latter critical segment comprise a buried α helix and two runs of antiparallel β sheet that constitute a contact face with their respective ubiquitin-like proteins. Therefore, truncation of

<sup>6</sup> Z. Tokgöz and A. L. Haas, unpublished observation.

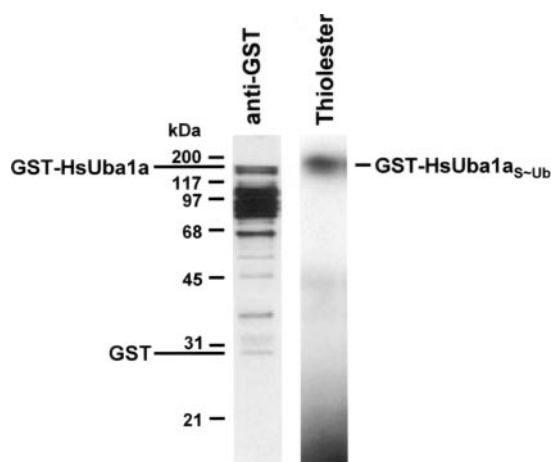


FIGURE 1. SDS-PAGE resolution of recombinant GST-HsUba1a. Left lane, glutathione-Sepharose affinity-purified human GST-HsUba1a was resolved by SDS-PAGE on a 7.5% gel under reducing conditions and then electrophoretically transferred to polyvinylidene difluoride membrane and visualized by Western blotting using affinity-purified rabbit anti-GST antibody and ECL detection. The migration positions for full-length GST-HsUba1a and free GST are shown to the left, along with mobility markers of the indicated molecular weights. Right lane, 1 pmol of wild type GST-HsUba1a was incubated in an end point <sup>125</sup>I-ubiquitin thiolester assay and then resolved in parallel by SDS-PAGE on the same gel as in the left lane but under nonreducing conditions (16). The GST-HsUba1a-<sup>125</sup>I-ubiquitin thiolester was visualized by autoradiography, the position of which is indicated to the right.

TABLE 1

## Stoichiometry of GST-HsUba1a ternary complexes

The end point formation of <sup>125</sup>I-ubiquitin thiolester to wild type or Asp<sup>576</sup> mutant GST-HsUba1a was determined in triplicate for a 1- or 20-min incubation, respectively, under conditions identical to those described in the legend of Fig. 2. The end point formation of ubiquitin [<sup>3</sup>H]adenylate bound to GST-Uba1a wild type or Asp<sup>576</sup> mutant was determined in triplicate by trichloroacetic acid-precipitable radioactivity for parallel incubations conducted identically to those for thiolester formation with the exception that reactions contained 1 μM [2,8-<sup>3</sup>H]ATP and 5 μM unlabeled ubiquitin (16, 17).

	<sup>125</sup> I-Ub thiolester	Ub [ <sup>3</sup> H]adenylate
	pmol	
GST-HsUba1a (wild type)	1.40 ± 0.10	1.32 ± 0.03
GST-HsUba1aD576A	0.80 ± 0.06	0.007 ± 0.001
GST-HsUba1aD576E	1.50 ± 0.06	0.008 ± 0.002
GST-HsUba1aD576N	0.40 ± 0.07	0.008 ± 0.001
GST-HsUba1aK528A	1.44 ± 0.07	0.002 ± 0.001

this segment reasonably explains complete inactivation of the enzyme by abolishing binding of the β-grasp polypeptide cosubstrate.

Parallel end point determinations of <sup>125</sup>I-ubiquitin thiolester and ubiquitin [<sup>3</sup>H]adenylate formation with wild type GST-HsUba1a were conducted as described under "Materials and Methods," the results of which are summarized in Table 1. The observed end point thiolester versus adenylate stoichiometry of 1.1 for the wild type GST-HsUba1a agreed well with the expected value of 1.0 reported for rabbit reticulocyte and human erythrocyte ubiquitin-activating enzymes (16, 27) and, more recently, for the human AppBp1-Uba3 heterodimer required for Nedd8 activation (29). These observations are important, since they indicate that the GST-HsUba1a degradation products are catalytically inactive within the resolution of the <sup>125</sup>I-ubiquitin thiolester and ubiquitin [<sup>3</sup>H]adenylate stoichiometry assays and, therefore, should not significantly contribute to subsequent kinetic studies conducted with either wild type or mutant fusion proteins.

**Recombinant GST-HsUba1a Shows Wild Type Kinetics**—We have previously shown that the kinetics for HsUba1-catalyzed transthiolation of HsUbc2b can be used as a reporter assay for determining the *K<sub>m</sub>* and *k<sub>cat</sub>* values for the three cosubstrates of the ubiquitin-activating enzyme (27). Similar studies monitoring the kinetics of HsUbc12-<sup>125</sup>I-

Nedd8 thiolester formation catalyzed by heterodimeric AppBp1-Uba3 demonstrate remarkable conservation in mechanism and cosubstrate affinities with respect to the ubiquitin-activating enzyme (29). Such E2 transthiolation assays are more sensitive to the potential presence of trace catalytically active fragments than the single turnover end point assays used for quantitating ternary complex stoichiometry, since the former require accumulation of product over multiple catalytic cycles. In this approach, the presence of two or more catalytically active species differing in *K<sub>m</sub>*, *k<sub>cat</sub>*, or both (as might be expected for degradation products of GST-HsUba1a) is indicated by deviation from strict hyperbolic kinetics and manifests as nonlinear double reciprocal plots of 1/*v<sub>o</sub>* versus 1/[substrate]<sub>o</sub> (30).

Initial velocity experiments with wild type GST-HsUba1a revealed strict hyperbolic kinetics based on the linearity of double reciprocal plots when ATP·Mg<sup>2+</sup>, <sup>125</sup>I-ubiquitin, or HsUbc2b was varied at saturating concentrations of the other cosubstrates (not shown). Values of *K<sub>m</sub>* and *k<sub>cat</sub>*, the latter defined as *V<sub>max</sub>*/[GST-HsUba1a]<sub>o</sub>, were calculated from nonlinear regression analyses of the respective data sets and are summarized in Table 2. In the presence of saturating <sup>125</sup>I-ubiquitin (5 μM) and recombinant HsUbc2b (0.5 μM), the *K<sub>m</sub>* of 5.5 ± 0.7 μM for ATP was in good agreement with the value of 7.0 ± 1.1 μM reported for wild type human erythrocyte Uba1 (27). Likewise, when [<sup>125</sup>I-ubiquitin]<sub>o</sub> was varied at saturating ATP·Mg<sup>2+</sup> (2 mM) and HsUbc2b (0.5 μM), wild type GST-HsUba1a exhibited a *K<sub>m</sub>* of 0.8 ± 0.1 μM for radiolabeled ubiquitin that was identical to that previously determined for human erythrocyte Uba1 (27). Finally, the concentration dependence for the initial rate of HsUbc2b transthiolation versus [HsUbc2b]<sub>o</sub> at saturating ATP·Mg<sup>2+</sup> (2 mM) and <sup>125</sup>I-ubiquitin (5 μM) yielded a *K<sub>m</sub>* of 111 ± 6 nM that was in excellent agreement with the value of 123 ± 19 nM determined earlier for the human erythrocyte enzyme (27). The intrinsic *k<sub>cat</sub>* for HsUbc2b transthiolation (*k<sub>cat,trans</sub>*) corresponded to 3.4 ± 0.1 s<sup>-1</sup> when calculated from the *V<sub>max</sub>* for GST-HsUba1a-catalyzed transthiolation in the latter experiment (Table 2) and agreed well with the value of 4.5 ± 0.3 s<sup>-1</sup> for erythrocyte HsUba1 (27).

The kinetic data demonstrate that the amino-terminal GST moiety has no measurable effect on the affinities of cosubstrate binding, reflected in the respective *K<sub>m</sub>* values, or the catalytic competence of the recombinant enzyme, reflected in the *k<sub>cat</sub>* values, since GST-HsUba1a was kinetically indistinguishable from the wild type activating enzyme isolated from human erythrocytes. This conclusion is in concordance with the similar end point stoichiometries for wild type and GST-HsUba1a ternary complexes (Table 1) and is understandable, since the predicted spatial orientation of the amino-terminal GST domain is well removed from the cosubstrate binding sites, based on the structure for human AppBp1-Uba3 and Sae1-Sae2 paralogs (22–24). More important, the strict hyperbolic kinetics exhibited by wild type GST-HsUba1a precludes significant contributions from the degradative fragments present in the recombinant enzyme preparations. Therefore, three independent lines of evidence indicate that only full-length GST-HsUba1a is catalytically active or, less likely, that the degradative fragments are kinetically indistinguishable from full-length enzyme. The latter conclusions allowed us unambiguously to examine the catalytic effects of the HsUba1a point mutants without necessitating resolution of full-length enzyme from the contaminating degradation products.

**Mutation of Asp<sup>576</sup> Decreases the Rate of Ubiquitin [<sup>3</sup>H]Adenylate Formation**—Earlier studies demonstrated that the stoichiometric formation of wild type Uba1 ternary complex is complete within the first 30 s of incubation with ATP·Mg<sup>2+</sup> and ubiquitin at 37 °C (16, 27, 29). Fig. 2 illustrates that ternary complex formation catalyzed by recombinant wild type GST-HsUba1a is also rapid at 2 mM ATP·Mg<sup>2+</sup> and 5 μM

TABLE 2

Summary of constants for GST-Uba1a kinetics

	$K_{m,ATP}$	$K_{m,Ub}$	$K_{m,HsUbc2b}$	$k_{cat,AMP-Ub}^a$	$k_{cat,trans}^b$
	<i>mM</i>	<i>mM</i>	<i>nM</i>	<i>s</i> <sup>-1</sup>	<i>s</i> <sup>-1</sup>
GST-HsUba1a (wild type)	5.5 ± 0.7	0.8 ± 0.1	111 ± 6	>6.0 ± 0.1	3.4 ± 0.1
GST-HsUba1aD576A	208 ± 15	29 ± 6	135 ± 36	0.024 ± 0.003	0.120 ± 0.010
GST-HsUba1aD576E	22 ± 3	1.1 ± 0.3	122 ± 30	0.005 ± 0.001	0.100 ± 0.010
GST-HsUba1aD576N	29 ± 6	4.0 ± 0.5	73 ± 4	0.011 ± 0.001	0.022 ± 0.001
GST-HsUba1aK528A	119 ± 17	2.3 ± 0.6	89 ± 9	0.015 ± 0.003	0.011 ± 0.001

<sup>a</sup> Intrinsic  $k_{cat}$  for ubiquitin adenylate formation corrected for saturating ATP and <sup>125</sup>I-ubiquitin.

<sup>b</sup> Intrinsic  $k_{cat}$  for HsUbc2b transthiolation corrected for saturating ATP, <sup>125</sup>I-ubiquitin, and HsUbc2b.

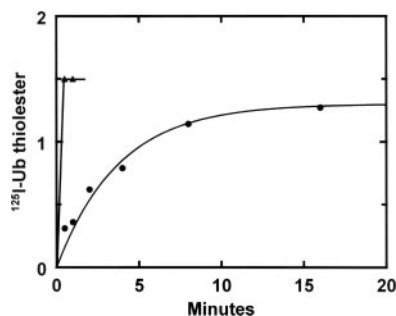


FIGURE 2. Time course for GST-HsUba1aD576A-<sup>125</sup>I-ubiquitin thiolester formation. The time course for <sup>125</sup>I-ubiquitin thiolester formation with 1.5 pmol (30 nM) of wild type GST-HsUba1a (closed triangles) per datum point or an equivalent amount of full-length GST-HsUba1aD576A (closed circles), determined by Coomassie staining following SDS-PAGE as in Fig. 1, was determined at 37 °C in 50- $\mu$ l incubations containing 50 mM Tris-HCl (pH 7.5), 2 mM ATP, 10 mM MgCl<sub>2</sub>, 1 mM DTT, 1 mg/ml carrier bovine serum albumin, and 5  $\mu$ M <sup>125</sup>I-ubiquitin (16, 17). Aliquots taken at the indicated times were quenched in 50  $\mu$ l of SDS sample buffer without  $\beta$ -mercaptoethanol and then resolved by nonreducing 7.5% SDS-PAGE and visualized by autoradiography. The absolute content of <sup>125</sup>I-ubiquitin thiolester was quantitated by  $\gamma$ -counting the excised bands for each time point and calculated using the specific activity of the radiolabeled polypeptide (16, 17). The line through the data for GST-HsUba1aD576A represents a theoretical first order fit for  $k_o = 0.005$  s<sup>-1</sup>.

<sup>125</sup>I-ubiquitin when measured as the corresponding <sup>125</sup>I-ubiquitin thiolester (closed triangles). A parallel assay confirmed that ubiquitin [<sup>3</sup>H]adenylate formation was stoichiometric with GST-HsUba1a-<sup>125</sup>I-ubiquitin thiolester at the earliest time point (30 s) in Fig. 2 (not shown), consistent with the results of Table 1 for the wild type recombinant enzyme. In contrast, <sup>125</sup>I-ubiquitin thiolester formation under identical conditions and with a nearly identical concentration of full-length GST-HsUba1aD576A, determined by end point <sup>125</sup>I-ubiquitin thiolester formation as described under "Materials and Methods," was markedly slower and required 20 min to reach completion (Fig. 2, closed circles). The time course for GST-HsUba1aD576A-<sup>125</sup>I-ubiquitin thiolester formation followed strictly first order kinetics over at least six half-lives, based on the linearity of appropriate semilog plots (not shown), and yielded a pseudo-first order rate constant of 0.005 s<sup>-1</sup>. In Fig. 2, the solid line through the data for GST-HsUba1aD576A (solid circles) represents a theoretical first order fit for  $k_o = 0.005$  s<sup>-1</sup>. The linearity of such first order plots precludes significant contributions from catalytically active degradation fragments having radically different kinetics, in agreement with conclusions drawn from the wild type stoichiometries of the recombinant enzyme preparations. Results qualitatively similar to those of Fig. 2 were obtained with the GST-HsUba1aD576E and GST-HsUba1aD576N mutants and yielded pseudo-first order rate constants of 0.003 and 0.006 s<sup>-1</sup>, respectively (not shown). These observations demonstrate that mutation at Asp<sup>576</sup> results in a  $\sim 10^3$ -fold reduction in the apparent first order rate constant for GST-HsUba1a-<sup>125</sup>I-ubiquitin thiolester formation compared with the lower limit of  $\sim 5$  s<sup>-1</sup> estimated previously for the intrinsic rate constant for ubiquitin [<sup>3</sup>H]adenylate formation catalyzed by wild type enzyme (27, 31).

**Mutation of Asp<sup>576</sup> Alters the Stoichiometry of HsUba1a Ternary Complex**—To determine the effect of each of the three point mutations on the stoichiometry for ternary complex formation, parallel incubations to those of Fig. 2 were conducted in the presence of 1  $\mu$ M [2,8-<sup>3</sup>H]ATP-Mg<sup>2+</sup> and 5  $\mu$ M unlabeled ubiquitin in order to determine HsUba1a-bound ubiquitin [<sup>3</sup>H]adenylate (16). No detectable ubiquitin [<sup>3</sup>H]adenylate intermediate was observed for any of the three mutants after 1 min at 37 °C, an incubation time during which wild type enzyme forms stoichiometric ubiquitin [<sup>3</sup>H]adenylate (16, 17, 29). However, the intermediate was marginally detectable after 5 min and reached an end point by 15 min, since no additional increase in ubiquitin [<sup>3</sup>H]adenylate was observed at 30 min (not shown). Table 1 summarizes equilibrium end point levels of <sup>125</sup>I-ubiquitin thiolester and ubiquitin [<sup>3</sup>H]adenylate for full-length GST-HsUba1aD576A, GST-HsUba1aD576E, and GST-HsUba1aD576N in parallel triplicate assays following incubation for 20 min at 37 °C. The amount of each mutant in the assays was normalized to that of full-length wild type GST-HsUba1a protein, as determined by Coomassie staining following SDS-PAGE resolution, so that the final <sup>125</sup>I-ubiquitin thiolester values reflect enzyme specific activity. End point values for <sup>125</sup>I-ubiquitin thiolester agreed reasonably well among wild type and mutant GST-HsUba1a when normalized to total full-length protein content (Table 1). Modest differences in enzyme-bound <sup>125</sup>I-ubiquitin thiolester formation among the four recombinant proteins probably reflect slight differences in the content of active enzyme within the preparations, since the variation is comparable with the yields of active enzyme observed among independent preparations of wild type GST-HsUba1a. Therefore, mutation of Asp<sup>576</sup> does not appear markedly to affect the end point formation of enzyme-bound <sup>125</sup>I-ubiquitin thiolester, although the data do not absolutely rule out small effects on the stoichiometry of this intermediate.

In contrast, the end point stoichiometries for the ubiquitin [<sup>3</sup>H]adenylate intermediate formed with each of the three mutants were only  $\sim 1\%$  of their respective thiolester values (Table 1). We have previously found that mutation of specific ubiquitin residues promotes dissociation of the otherwise tightly enzyme-bound ubiquitin [<sup>3</sup>H]adenylate and its subsequent hydrolysis by contaminating ubiquitin carboxyl-terminal hydrolases (31). In the present case, the apparent substoichiometric ubiquitin [<sup>3</sup>H]adenylate formation did not arise by similar dissociation of the intermediate from the enzyme and cleavage by any contaminating hydrolases, since exogenous free ubiquitin [<sup>3</sup>H]adenylate prepared by trichloroacetic acid precipitation of wild type Uba1 ternary complex (16, 18) was stable when added to the recombinant GST-HsUba1a mutant preparations (not shown). Previous kinetic studies have demonstrated that formation of enzyme-bound ubiquitin adenylate is rapid and that the subsequent transfer to form the covalent Uba1-ubiquitin thiolester is the rate-limiting step of ternary complex formation with the wild type enzyme (16, 17). This accounts for the constant 1:1 stoichiometry of thiolester/adenylate with time (16, 17). That ubiquitin [<sup>3</sup>H]adenylate is undetectable during the first 5 min of the time course in Fig. 2 and remains at only 1% of the end point thiolester for the three

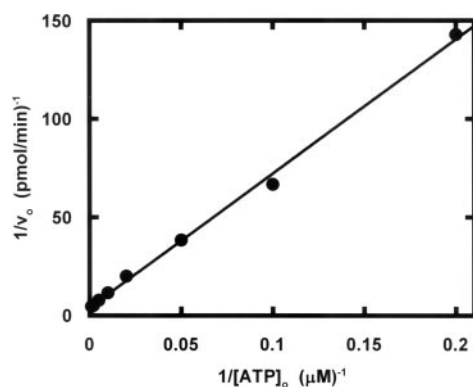


FIGURE 3. **Hyperbolic dependence for the initial velocity of GST-HsUba1aD576A-<sup>125</sup>I-ubiquitin thiolester formation on ATP concentration.** Initial rates of GST-HsUba1aD576A-<sup>125</sup>I-ubiquitin thiolester formation were determined at 37 °C in 1-min incubations of 25- $\mu$ l total volume containing 50 mM Tris-HCl (pH 7.5), 10 mM MgCl<sub>2</sub>, 1 mM DTT, 1 mg/ml carrier bovine serum albumin, 10  $\mu$ M <sup>125</sup>I-ubiquitin, 52 nM GST-HsUba1aD576A, and the indicated concentrations of ATP as described previously (16, 27). A hyperbolic concentration dependence with respect to ATP concentration was confirmed by linearity of the corresponding double reciprocal plot. Relevant kinetic constants were determined by nonlinear regression (27).

Asp<sup>576</sup> mutants requires that under the conditions of the assay, ubiquitin [<sup>3</sup>H]adenylate formation must be rate-limiting and that the mutations have altered the equilibrium constant for formation of this intermediate.

**Effect of Asp<sup>576</sup> Mutants on GST-HsUba1a Thiolester Kinetics**—Because mutation of Asp<sup>576</sup> shifts the rate-limiting step of GST-HsUba1a ternary complex formation to that of ubiquitin adenylate formation, we used a similar kinetic approach to that for wild type enzyme but instead directly monitored formation of GST-HsUba1a-<sup>125</sup>I-ubiquitin thiolester. If Asp<sup>576</sup> of GST-HsUba1a interacts with the chelated metal of ATP·Mg<sup>2+</sup>, then mutation of this residue to alanine is predicted minimally to decrease the affinity for ATP·Mg<sup>2+</sup> binding, reflected in an increased  $K_m$ . Fig. 3 demonstrates that the dependence of the initial rates for <sup>125</sup>I-ubiquitin thiolester formation to GST-HsUba1aD576A with respect to [ATP]<sub>0</sub> follows simple hyperbolic kinetics in the presence of 10  $\mu$ M <sup>125</sup>I-ubiquitin, as shown by the linearity of the corresponding reciprocal plot. Nonlinear regression analysis of the data yielded a  $K_m$  of  $208 \pm 15 \mu$ M for ATP·Mg<sup>2+</sup> that represented a 38-fold increase over that for wild type GST-HsUba1a (Table 2). The  $V_{max}$  value from Fig. 3 corresponded to a  $k_{cat}$  of  $0.0035 \pm 0.0001 \text{ s}^{-1}$  that agreed well with the first order rate constant of  $0.005 \text{ s}^{-1}$  determined in Fig. 2 at saturating ATP·Mg<sup>2+</sup> and an identical concentration of radioiodinated ubiquitin. The increase in  $K_m$  for GST-HsUba1aD576A is consistent with the predicted role for Asp<sup>576</sup> in binding ATP·Mg<sup>2+</sup> within the adenylate active site. Table 2 also summarizes  $K_m$  values obtained for GST-HsUba1aD576E and GST-HsUba1aD576N mutants in experiments parallel to those of Fig. 3. The relatively conservative D576E mutation results in a much less dramatic 4-fold increase in  $K_m$  for ATP·Mg<sup>2+</sup> binding compared with wild type GST-HsUba1a, presumably reflecting the influence of the longer glutamate side chain. The side chain amide of asparagine is relatively efficient in substituting for the carboxyl function of Asp<sup>576</sup>, since the D576N point mutant yields a similar 5-fold increase in  $K_m$  for ATP·Mg<sup>2+</sup> (Table 2). The apparent  $k_{cat}$  values at 5  $\mu$ M <sup>125</sup>I-ubiquitin of  $0.006 \pm 0.001$  and  $0.005 \pm 0.001 \text{ s}^{-1}$  derived from the respective  $V_{max}$  for the D576E and D576N mutants (not shown) were in good agreement with the corresponding first order rate constants obtained from kinetic studies similar to those of Fig. 2.

Since Asp<sup>576</sup> functions in ATP·Mg<sup>2+</sup> binding, confirmed by the results of Fig. 3 and Table 2, we did not *a priori* expect to observe an effect of the Asp<sup>576</sup> mutations on ubiquitin binding. However, mutation

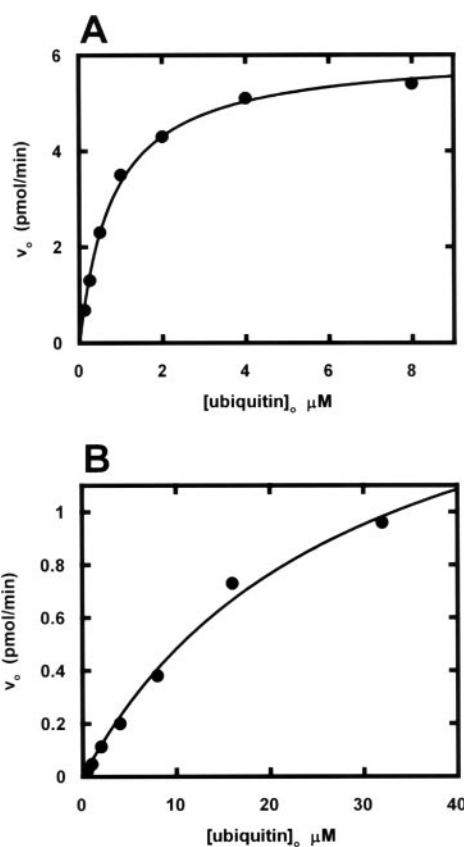


FIGURE 4. **Hyperbolic <sup>125</sup>I-ubiquitin concentration dependence for wild type and Asp<sup>576</sup> mutant GST-HsUba1a.** A, initial rates of wild type GST-HsUba1a-catalyzed HsUbc2b-<sup>125</sup>I-ubiquitin thiolester formation were determined in 30-s incubations under the conditions described in the legend to Fig. 3 except that [ATP]<sub>0</sub> was held at 2 mM and <sup>125</sup>I-ubiquitin was present at the indicated concentrations. B, initial rates for GST-HsUba1aD576A-<sup>125</sup>I-ubiquitin thiolester formation were determined in 1-min incubations identical to those described in the legend to Fig. 3, except that [ATP]<sub>0</sub> was held constant at 2 mM and <sup>125</sup>I-ubiquitin was present at the indicated concentrations. Lines through the data represent hyperbolic nonlinear regression fits from which the relevant constants summarized in Table 2 were determined.

of Asp<sup>576</sup> to alanine significantly reduced the affinity of the point mutant for <sup>125</sup>I-ubiquitin (Fig. 4B) relative to that exhibited by wild type GST-HsUba1a (Fig. 4A) and yielded a  $K_m$  of  $29 \pm 6 \mu$ M (Table 2) when measured by the initial rate of GST-HsUba1aD576A-<sup>125</sup>I-ubiquitin thiolester formation at saturating ATP (2 mM). The  $V_{max}$  from Fig. 4B yielded a  $k_{cat}$  of  $0.024 \pm 0.003 \text{ s}^{-1}$ , which must represent the intrinsic first order rate constant for <sup>125</sup>I-ubiquitin adenylate formation ( $k_{cat,AMP-Ub}$ ) (Table 2). In contrast, mutation of Asp<sup>576</sup> to asparagine increased the  $K_m$  for ubiquitin binding to GST-HsUba1aD576N only 5-fold ( $K_m = 4.0 \pm 0.5 \mu$ M) and yielded a corresponding  $k_{cat,AMP-Ub}$  of  $0.011 \pm 0.001 \text{ s}^{-1}$ , Table 2. Although the GST-HsUba1aD576E point mutant showed no significant effect on the binding of <sup>125</sup>I-ubiquitin when measured as  $K_m$ , the relatively conservative point mutation exhibited the greatest effect on  $k_{cat,AMP-Ub}$  for ubiquitin adenylate formation ( $0.005 \pm 0.001 \text{ s}^{-1}$ ) (Table 2), suggesting that the increase in side chain length for glutamate has a substantial effect on formation of the transition state for enzyme-bound ubiquitin adenylate. The results of Table 2 indicate that mutation of Asp<sup>576</sup> has a much less dramatic effect on the binding of ubiquitin within the HsUba1a adenylate active site than found for binding of ATP·Mg<sup>2+</sup> and that this effect is qualitatively proportional to the extent to which the mutations ablate ATP·Mg<sup>2+</sup> binding. In contrast, the ability of HsUba1a to catalyze ubiquitin adenylate formation is markedly sensitive to mutation at Asp<sup>576</sup>, implicating this residue in transition state stabilization of this step.

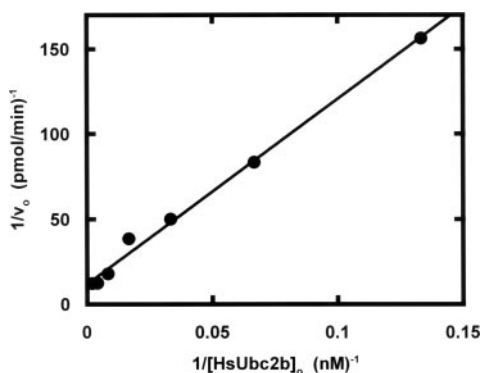


FIGURE 5. Dependence of initial velocity on HsUbc2b concentration for GST-HsUba1aD576A-catalyzed HsUbc2b transthiolation. Initial rates of GST-HsUba1aD576A-catalyzed HsUbc2b-<sup>125</sup>I-ubiquitin thiolester formation were determined in 25- $\mu$ l incubations at 37 °C for 10 min in assays containing 50 mM Tris-HCl (pH 7.5), 2 mM ATP, 10 mM MgCl<sub>2</sub>, 1 mM DTT, 1 mg/ml carrier bovine serum albumin, 2.5 nM GST-HsUba1aD576A, 10  $\mu$ M <sup>125</sup>I-ubiquitin, and the indicated concentrations of HsUbc2b (27). Hyperbolic binding kinetics were confirmed by the linearity of the corresponding double reciprocal plot. Values for  $K_m$  and  $V_{max}$  values were calculated by nonlinear hyperbolic regression analysis and are summarized in Table 2.

**Effect of Asp<sup>576</sup> Mutants on GST-HsUba1a-catalyzed Transthiolation Kinetics**—Previous studies have shown that transthiolation within the Michaelis complex comprising HsUbc2b bound to the HsUba1a ternary complex represents the rate-limiting step for HsUbc2b charging (27). The Asp<sup>576</sup> point mutants catalyzed significantly slower rates of HsUbc2b transthiolation, as expected for rate-limiting ubiquitin adenylate formation revealed from earlier experiments (Table 2). Initial rates of GST-HsUba1a mutant-catalyzed HsUbc2b-<sup>125</sup>I-ubiquitin thiolester formation were measured at 2 mM ATP and 10  $\mu$ M <sup>125</sup>I-ubiquitin in the presence of increasing concentrations of HsUbc2b. The resulting data exhibited a hyperbolic concentration dependence with respect to [HsUbc2b]<sub>0</sub> for all three point mutants based on the linearity of the corresponding reciprocal plot, representative data for which is shown for GST-HsUba1aD576A in Fig. 5. Relevant kinetic constants were calculated from the data by nonlinear hyperbolic regression analysis and are also summarized in Table 2.

The three Asp<sup>576</sup> point mutants exhibited  $K_m$  values for HsUbc2b binding that were in good agreement with that found for wild type GST-HsUba1a (Table 2), indicating that this residue does not contribute either directly or indirectly to HsUbc2b binding. The corresponding apparent  $k_{cat}$  values for HsUbc2b transthiolation were calculated from  $V_{max}/[GST-HsUba1a\ mutant]_0$ . We anticipated that the intrinsic  $k_{cat}$  for HsUbc2b transthiolation ( $k_{cat,trans}$ ), when corrected for saturating [ATP]<sub>0</sub> and [ubiquitin]<sub>0</sub>, would correspond to the intrinsic  $k_{cat,AMP-Ub}$  values determined for mutant-bound ubiquitin adenylate formation, since the latter represented the rate-limiting step for ternary complex formation and, therefore, the rate-limiting step for subsequent HsUbc2b-<sup>125</sup>I-ubiquitin thiolester formation. However, the three mutants exhibited intrinsic  $k_{cat,trans}$  values that were statistically greater than  $k_{cat,AMP-Ub}$  (Table 2). In the presence of GST-HsUba1aD576A,  $k_{cat,trans}$  for HsUbc2b transthiolation ( $0.120 \pm 0.010\ s^{-1}$ ) was ~5-fold greater than the  $k_{cat,AMP-Ub}$  for the corresponding ubiquitin adenylate formation. The GST-HsUba1aD576E and GST-HsUba1aD576N mutants also catalyzed greater intrinsic rates of HsUbc2b transthiolation than predicted from their corresponding values of  $k_{cat,AMP-Ub}$  for ubiquitin adenylate formation (Table 2). The  $k_{cat,trans}$  for the D576E mutant ( $0.100 \pm 0.010\ s^{-1}$ ) was 20-fold greater than  $k_{cat,AMP-Ub}$  ( $0.005 \pm 0.001\ s^{-1}$ ), whereas the D576N mutant exhibited a 2-fold greater  $k_{cat,trans}$  (Table 2). These differences suggest that HsUbc2b transthiolation enhances the rate of ubiquitin adenylate formation. This

effect is not due to allosteric activation by HsUbc2b binding alone, since substitution of 0.5  $\mu$ M HsUbc2bC88A, which is incapable of forming a thiolester (27), did not result in a measurable increase in  $k_{cat,AMP-Ub}$  with GST-HsUba1aD576A (not shown). Therefore, the stimulation in observed  $k_{cat}$  requires the active site Cys<sup>88</sup> of HsUbc2b.

**Mutation of Asp<sup>576</sup> Alters the Mechanism of Co-substrate Binding for GST-HsUba1a**—The mechanism of ubiquitin activation by rabbit reticulocyte Uba1 exhibits absolutely ordered binding in which ATP·Mg<sup>2+</sup> is the leading and ubiquitin the trailing substrate (17). Ordered binding typically implies the presence of an obligatory conformational change upon binding of the leading substrate that allows the subsequent binding of the trailing substrate. Paradoxically, the observation that selected ubiquitin point mutants support random addition mechanisms with wild type Uba1 indicates that ordered substrate addition and the presumed conformational change are not requisites for the catalytic cycle of ubiquitin activation (31). This conclusion is supported by our recent finding that the catalytic cycle of Nedd8 activation by heterodimeric AppBp1-Uba3 follows a pseudo-ordered but formally random mechanism in which ATP·Mg<sup>2+</sup> is the preferred leading substrate, although Nedd8 is capable of binding first at high concentrations (29). The effects of the Asp<sup>576</sup> mutations on the binding affinities for ATP and ubiquitin suggested that the mechanism of substrate addition might also be affected. To test this prediction, ATP/<sup>32</sup>PP<sub>i</sub> isotope exchange kinetics were used to examine the order of substrate addition among wild type GST-HsUba1a and the three Asp<sup>576</sup> point mutants.

Wild type GST-HsUba1a and the Asp<sup>576</sup> point mutants exhibited hyperbolic kinetics for their dependence of the initial rate for ATP/<sup>32</sup>PP<sub>i</sub> exchange on [ATP]<sub>0</sub> (data not shown). When the ubiquitin concentration was varied at a constant ATP concentration (2 mM), wild type GST-HsUba1a showed hyperbolic behavior below 2  $\mu$ M ubiquitin, indicated by the linearity of the corresponding double reciprocal plot (not shown), and yielded an estimated  $K_{1/2}$  of  $0.17 \pm 0.01\ \mu$ M and an extrapolated  $V_{max}$  of  $65 \pm 1\ \text{pmol/min}$  ( $k_{cat} = 6.0 \pm 0.1\ s^{-1}$ ). However, substrate inhibition was observed at higher ubiquitin concentrations that tended to a limiting initial rate of 5 pmol/min, representing 8% of the extrapolated  $V_{max}$  (Fig. 6A). This indicates that human Uba1a exhibits a pseudo-ordered mechanism for substrate binding, with ATP·Mg<sup>2+</sup> being the preferred leading substrate and ubiquitin the preferred trailing substrate (17). In contrast, hyperbolic kinetics were observed at all ubiquitin concentrations tested for GST-HsUba1aD576A (Fig. 6B) and GST-HsUba1aD576E (Fig. 6C), demonstrating that the point mutations shift the enzyme to a purely random addition mechanism for substrate binding. The D576A mutant had the most dramatic effect on the isotope exchange kinetics, shifting the concentration dependence to near linearity, from which we could only estimate a lower limit to the  $K_{1/2}$  of  $5 \pm 2\ \text{mM}$  and a  $k_{cat}$  of  $0.7 \pm 0.9\ s^{-1}$ .<sup>7</sup> Although  $K_{1/2}$  cannot be directly equated with the corresponding  $K_m$  value, as has been discussed previously (31), the marked increase in  $K_{1/2}$  for GST-HsUba1aD576A is consistent with the significantly larger  $K_m$  for ATP (Table 2). The effect of the D576E mutant was much less severe and yielded a  $K_{1/2}$  of  $283 \pm 12\ \mu$ M and a  $k_{cat}$  of  $1.3 \pm 0.1\ s^{-1}$ . We cannot preclude substrate inhibition for the Asp<sup>576</sup> mutants at higher ubiquitin concentrations than those tested in Fig. 6, B and C; however, since substrate inhibition is apparent within 2-fold of the  $K_{1/2}$  for wild type GST-HsUba1a, it is unlikely that the point mutants would show similar substrate inhibition at still higher concentrations. These results indicate that coordination of Asp<sup>576</sup> with the metal of ATP·Mg<sup>2+</sup> is coupled to events in the adenylate active site

<sup>7</sup> The atypically large S.E. values for these kinetic constants reflect the problem associated with fitting a hyperbolic curve over a limited range near or below the inflection point (17).

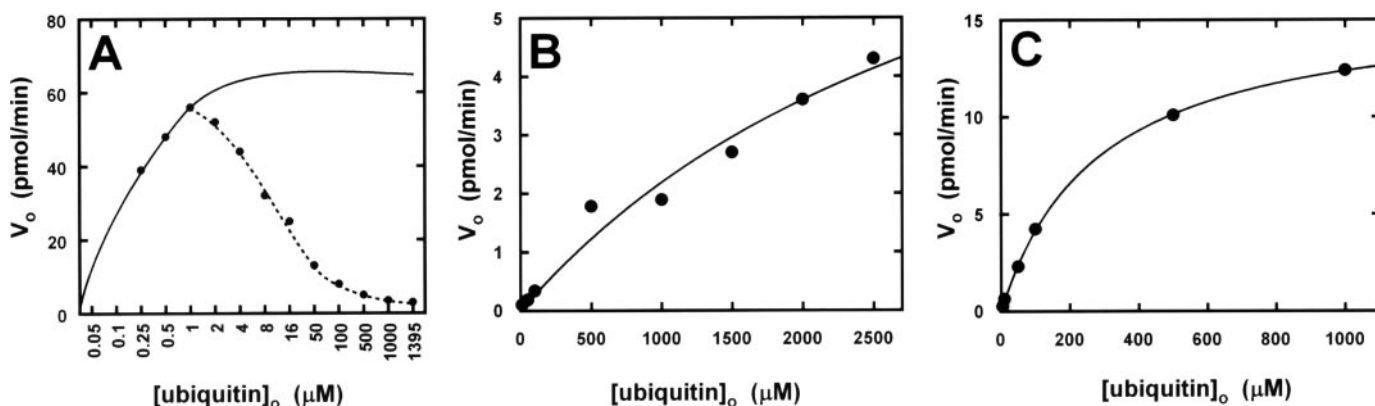


FIGURE 6. Dependence of ubiquitin concentration on the initial rate of GST-HsUba1a-catalyzed ATP/PP<sub>i</sub> exchange. Initial velocities of ATP/<sup>32</sup>P<sub>i</sub> exchange were determined at 37 °C in 50- $\mu$ l incubations containing 50 mM Tris-HCl (pH 7.5), 2 mM ATP, 10 mM MgCl<sub>2</sub>, 0.1 mM <sup>32</sup>P<sub>i</sub>, 1 mM DTT, the indicated concentrations of ubiquitin, and either GST-HsUba1a or Asp<sup>576</sup> mutant (17). A, ubiquitin dependence for wild type GST-HsUba1a (3.6 nM); B, ubiquitin dependence for GST-HsUba1aD576A (3.2 nM); C, ubiquitin dependence for GST-HsUba1aD576E (4 nM). The solid lines represent nonlinear hyperbolic regression fits.

responsible for pseudo-ordered substrate addition, providing a mechanistic insight not apparent from the extant crystal structures for this enzyme family.

**Mutation of Lys<sup>528</sup> Mimics the Kinetic Phenotype of Asp<sup>576</sup> Alteration**—The complex kinetic phenotype of the Asp<sup>576</sup> mutants suggests that ATP·Mg<sup>2+</sup> and ubiquitin binding are functionally coupled in the catalytic cycle of ubiquitin activation. To distinguish whether this effect specifically results from coordination of Asp<sup>576</sup> to Mg<sup>2+</sup> or is a more generalized effect of ATP·Mg<sup>2+</sup> binding, we examined the consequence of mutating Lys<sup>528</sup> to alanine. Lysine 528 is predicted to hydrogen-bond to the  $\beta$ -phosphoryl oxygen of ATP·Mg<sup>2+</sup>, as it does for Lys<sup>86</sup> of bacterial MoeB, Lys<sup>103</sup> of human Uba3, and Lys<sup>72</sup> of human Sae2 (21, 23, 24). We find that the phenotype for Lys<sup>528</sup> mutation is remarkably similar to that of the Asp<sup>576</sup> mutants. The time course for GST-HsUba1aK528A-<sup>125</sup>I-ubiquitin thiolester formation was exponential, with a  $k_o = 0.005$  s<sup>-1</sup>, similar to that observed for GST-HsUba1aD576A (Fig. 2), and yielded a ternary complex at equilibrium having thiolester that was approximately stoichiometric with the estimated protein content but a much attenuated ubiquitin [<sup>3</sup>H]adenylate level (Table 1).

The kinetics of GST-HsUba1aK528A-<sup>125</sup>I-ubiquitin thiolester formation were determined in parallel to those of the Asp<sup>576</sup> point mutants, the results of which are summarized in Table 2. Mutation of Lys<sup>528</sup> lowers the affinity for ATP·Mg<sup>2+</sup> somewhat less than mutating Asp<sup>576</sup> to alanine but consistent with the predicted contribution of the Lys<sup>528</sup> hydrogen bond to the  $\beta$ -phosphoryl oxygen of ATP·Mg<sup>2+</sup>. The Lys<sup>528</sup> mutation also slightly alters the affinity for ubiquitin (Table 2). Like the Asp<sup>576</sup> mutants, GST-HsUba1aK528A exhibits a wild type affinity for HsUbc2b (Table 2). Finally, in ATP/PP<sub>i</sub> isotope exchange assays similar to those of Fig. 6, GST-HsUba1aK528A exhibited purely hyperbolic kinetics with respect to [ubiquitin]<sub>o</sub>, indicating random substrate addition (not shown). These results are consistent with the kinetic phenotypes of the Asp<sup>576</sup> and Lys<sup>528</sup> mutants arising by a generalized effect on ATP·Mg<sup>2+</sup> binding.

## DISCUSSION

The present studies demonstrate for the first time that alterations in the ATP·Mg<sup>2+</sup> binding site of Uba1 exhibit a remarkably pleiotropic phenotype in the activation of ubiquitin that could not have been anticipated from the crystal structures currently available for members of the E1 superfamily. Lake *et al.* (21) originally proposed that Asp<sup>130</sup> of MoeB contributed to ATP binding by interacting with the chelated Mg<sup>2+</sup>, supported by the loss-of-function phenotype in nitrate reductase over-*lay* assays when this group was mutated to alanine. Paralogous mutation

of Asp<sup>146</sup> within the Uba3 subunit of human Nedd8-activating enzyme supported this functional role, since it abrogated <sup>32</sup>P-labeled Nedd8 adenylate formation and subsequent thiolester formation at the active site Cys<sup>216</sup> of Uba3 (22). Similar observations have been made following mutation of Asp<sup>117</sup> of Sae2 within the human Sae1-Sae2 heterodimeric activating enzyme for Sumo (24). Finally, the structure for ATP·Mg<sup>2+</sup> bound to SAE1-SAE2 is consistent with coordination of the conserved aspartate with the chelated metal (24). Collectively, these results suggest a central role for this residue in the mechanism of these enzymes, presumably reconciled by its predicted contribution to ATP·Mg<sup>2+</sup> binding. However, given the high affinity with which members of the E1 superfamily bind ATP·Mg<sup>2+</sup> (17, 27, 29), the observed loss-of-function phenotypes for these mutations require abrogation of ATP·Mg<sup>2+</sup> binding, which is difficult to reconcile with additional interactions between the nucleotide and its binding site. In the present paper, we quantitatively demonstrate the contribution of Asp<sup>576</sup> of human Uba1 to the affinity of ATP·Mg<sup>2+</sup> binding within the adenylate active site; more importantly, the data show that Asp<sup>576</sup> is critical to downstream events in the catalytic cycle of ubiquitin activation that instead account for the loss-of-function phenotype.

Wild type human Uba1a has a marked affinity for ATP ( $K_m = 5.5 \pm 0.7$   $\mu$ M), corresponding to a  $\Delta G_{\text{binding}}$  of 7.2 kcal/mol, presumably ensuring that the rate of ubiquitin activation is independent of fluctuations in this cosubstrate (4). The affinity of human Uba1 for ATP is reduced 38-fold by mutation of Asp<sup>576</sup> to alanine ( $K_m = 208 \pm 15$   $\mu$ M) (Table 2), an effect that is consistent with the proposed role of this residue in coordinating with the chelated metal of ATP·Mg<sup>2+</sup> (21, 24) but insufficient to produce a loss-of-function phenotype at millimolar intracellular nucleotide concentrations (32). The increase in  $K_m$  for ATP binding between the wild type and D576A mutant corresponds to a  $\Delta\Delta G_{\text{binding}}$  contribution of 2.1 kcal/mol for Asp<sup>576</sup>, much less than the total binding energy of the nucleotide.<sup>8</sup> The residual binding affinity of the Asp<sup>576</sup> point mutant requires additional contributions from other active site interactions. The Lys<sup>528</sup>- $\beta$ -phosphoryl hydrogen bond inferred from crystal structures (21, 23, 24) accounts for one of these interactions, since mutation of this residue to alanine results in a  $K_m$  of  $119 \pm 17$   $\mu$ M (Table 2), representing a  $\Delta\Delta G_{\text{binding}}$  of 1.8 kcal/mol. By comparison, *Bacillus stearothermophilus* tyrosyl-tRNA synthetase catalyzes a biochemically analogous ATP-coupled carboxyl group activation during the formation of a high energy tyrosyl adenylate intermedi-

<sup>8</sup> Binding energy estimates calculated from the corresponding  $\Delta\Delta G_{\text{binding}}$  values are not strictly additive due to entropic contributions.

## ATP·Mg<sup>2+</sup> Binding to the Ubiquitin-activating Enzyme

ate. Lysine 82 of the enzyme hydrogen-bonds to the  $\beta$ -phosphoryl oxygen of ATP·Mg<sup>2+</sup>, and mutation of this group to alanine yields a  $\Delta\Delta G_{\text{binding}}$  of 1.3 kcal/mol (33). Therefore, the binding contribution of Lys<sup>528</sup> within the HsUba1a nucleotide binding site is consistent with related active site interactions.

Much smaller effects on ATP·Mg<sup>2+</sup> binding affinity of ~5-fold, corresponding to  $\Delta\Delta G_{\text{binding}}$  values of 0.8 or 1.0 kcal, are observed when Asp<sup>576</sup> is mutated to either glutamate or asparagine, respectively (Table 2). The reduced binding of GST-HsUba1aD576E probably arises from steric constraints imposed by the longer side chain of glutamate in its interaction with bound ATP·Mg<sup>2+</sup>. The  $\Delta\Delta G_{\text{binding}}$  of 1.0 kcal/mol for GST-Uba1aD576N approximates a value of 1.7 kcal/mol for the difference in GTP·Mg<sup>2+</sup> binding within the G domain of EF-Tu following mutation of Asp<sup>80</sup>, a residue that similarly binds the Mg<sup>2+</sup> of the nucleotide chelate (34). That asparagine substitutes remarkably well for Asp<sup>576</sup> with respect to ATP·Mg<sup>2+</sup> binding suggests that interaction of the latter with chelated Mg<sup>2+</sup> is not due to Coulombic contributions. Coordination of asparaginyl and glutaminyl side chains to Mg<sup>2+</sup> have been observed previously for wild type enzymes, such as bacterial glutathione synthetase, D-alanine, D-alanine ligase, and pyruvate phosphate dikinase, among others (35, 36).

Several lines of evidence demonstrate that mutating Asp<sup>576</sup> alters the rate-limiting step for generating the HsUba1a ternary complex from the step for formation of the HsUba1a-ubiquitin thiolester to that of ubiquitin adenylate (Tables 1 and 2). For wild type ubiquitin-activating enzyme, generation of the ternary complex containing both HsUba1a-ubiquitin thiolester and its tightly bound ubiquitin adenylate precursor is rapid with respect to E2 transthiolation (27, 29). However, mutation of Asp<sup>576</sup> significantly reduces the rate of ubiquitin adenylate formation and allows the time course for HsUba1a ternary complex formation to be observed directly (Fig. 2). That the effect of Asp<sup>576</sup> mutation is at the step of ubiquitin adenylate formation and not the subsequent step of HsUba1a-ubiquitin thiolester formation is supported by the marked change in end point stoichiometry for wild type *versus* mutant ternary complex with the three substitutions tested (Table 1).

The kinetic assays are unable directly to resolve the intrinsic rate constant for  $k_{\text{cat,AMP-Ub}}$  on the step for ubiquitin adenylate formation catalyzed by wild type Uba1 (17). However, a lower limit for wild type  $k_{\text{cat,AMP-Ub}}$  of  $6.0 \pm 0.1 \text{ s}^{-1}$  can be estimated from the extrapolated  $k_{\text{cat}}$  for ATP/PP<sub>i</sub> isotope exchange at saturating ATP·Mg<sup>2+</sup> and ubiquitin (Fig. 6A), which agrees well with the lower limit of  $9.6 \text{ s}^{-1}$  determined for rabbit Uba1 (17).<sup>9</sup> Using the former limiting value, mutation of Asp<sup>576</sup> to alanine results in a >250-fold decrease in  $k_{\text{cat,AMP-Ub}}$  relative to wild type enzyme (Table 2). The overall effect of mutating Asp<sup>576</sup> can be quantitatively compared by considering the catalytic specificity of HsUba1a with respect to ATP·Mg<sup>2+</sup>, defined as  $k_{\text{cat,AMP-Ub}}/K_{m,\text{ATP}}$ . For wild type GST-HsUba1a, the lower limit for  $k_{\text{cat,AMP-Ub}}/K_{m,\text{ATP}}$  can be estimated as  $1.1 \times 10^6 \text{ M}^{-1} \text{ s}^{-1}$ , whereas the corresponding value for GST-HsUba1aD576A is  $115 \text{ M}^{-1} \text{ s}^{-1}$ . The consequence of the mutating Asp<sup>576</sup> to alanine thus represents a >9600-fold decrease in the overall efficiency of ubiquitin adenylate formation, an effect that renders HsUba1a functionally inactive under all but the most sensitive assay conditions. This suggests that the loss-of-function phenotype observed for the paralogous mutation in other members of this family results from a combination of reduced affinity and compromised catalytic efficiency (21, 23, 24). Reduction in  $k_{\text{cat,AMP-Ub}}$  also manifests as a

significantly diminished equilibrium constant for ubiquitin adenylate formation, normally ~0.1 for wild type enzyme (17, 37), since it constitutes the numerator of this term (17), altering the end point stoichiometry for the resulting HsUba1a ternary complex (Table 1).

We could not have anticipated *a priori* that mutation of Asp<sup>576</sup> or Lys<sup>528</sup> would so dramatically lower  $k_{\text{cat,AMP-Ub}}$  and the stoichiometry for the final ternary complex. Aspartate 576 is unlikely to serve an overt catalytic role as a general acid-base group, since glutamate does not effectively substitute for Asp<sup>576</sup> with respect to the stoichiometry of the ternary complex or the magnitude of  $k_{\text{cat,AMP-Ub}}$  (Tables 1 and 2). A functional ternary complex of correct stoichiometry can be reconstituted by the addition of exogenous ubiquitin adenylate to wild type Uba1 (18), even when enzyme and ubiquitin adenylate are both treated with 20 mM EDTA; therefore, we can preclude an alternative model for Asp<sup>576</sup> in which Mg<sup>2+</sup> remains associated with this residue to facilitate nucleophilic attack of Cys<sup>632</sup> during subsequent Uba1-ubiquitin thiolester formation. However, because the phenotype of Lys<sup>528</sup> mutation is similar to that observed with the three Asp<sup>576</sup> mutants, it is likely that they all derive from a common mechanism.

Aminoacyl tRNA synthetases catalyze a carboxyl group activation that is identical in chemistry to the reaction of Uba1 and other E1 paralogs (16, 38). These enzymes catalyze a highly conserved in line nucleophilic attack of the substrate carboxyl group on the  $\alpha$ -phosphate of ATP·Mg<sup>2+</sup> to form the corresponding bound aminoacyl adenylate and PP<sub>i</sub>·Mg<sup>2+</sup> (38–40). The reaction passes through a trigonal bipyramidal pentacoordinate phosphoryl transition state in which the relative positions of the oxygen and phosphorous atoms are proposed to shift little from their ground states (38, 39). Catalysis in this enzyme class arises in large part from enhanced binding and concomitant stabilization of the incipient transition state (38, 41, 42). Thus, mutation of active site groups involved in substrate binding that are also critical for binding and stabilizing the transition state invariably leads to marked reductions in  $k_{\text{cat}}$  (42, 43). As a corollary, mutation of groups not involved in initial substrate binding but that are required for transition state stabilization also shows significant  $k_{\text{cat}}$  effects (42, 43).

For HsUba1a, the significant decrease in  $k_{\text{cat,AMP-Ub}}$  requires, by definition, that the effect of mutating Asp<sup>576</sup> and Lys<sup>528</sup> groups in the ATP·Mg<sup>2+</sup> binding site results in destabilization of the transition state. Thus, the data of Table 2 suggest that mutation of Asp<sup>576</sup> destabilizes the transition state by 1.2 kcal/mol for HsUba1aD576A, 2.1 kcal/mol for HsUba1aD576E, and 1.4 kcal/mol for HsUba1aK528A (Table 2). The latter energy of destabilization agrees favorably with a value for  $\Delta\Delta G^\ddagger$  of 1.7 kcal/mol for mutation of Lys<sup>82</sup> to alanine in tyrosyl-tRNA synthetase noted earlier (33). Therefore, the common chemistries of these otherwise unrelated enzyme classes appear to manifest a conserved catalytic mechanism of transition state stabilization.

Ternary complex formation is normally too rapid to follow by the manual assays used in the present studies, necessitating our use of E2 transthiolation as a coupled reporter assay (27). Since mutation of Asp<sup>576</sup> or Lys<sup>528</sup> inhibits formation of bound ubiquitin adenylate, we were able to monitor subsequent HsUba1a-<sup>125</sup>I-ubiquitin thiolester formation directly (Fig. 2). Thus,  $V_{\text{max}}$  determined under these conditions and extrapolated to saturating substrate reflects the intrinsic value of  $k_{\text{cat,AMP-Ub}}$  for the respective single point mutants (Table 2). Because kinetics measure only the rate-limiting reaction of a multistep pathway, in this case ubiquitin adenylate formation, we were surprised to find that  $k_{\text{cat,trans}}$  values independently determined by HsUbc2b transthiolation failed to agree with those determined directly by HsUba1a-<sup>125</sup>I-ubiquitin thiolester formation (Table 2). Observation that the dominant negative mutant HsUbc2bC88A failed to enhance  $k_{\text{cat,AMP-Ub}}$  rules out

<sup>9</sup> Since ubiquitin adenylate formation is not rate-limiting for wild type E1 ternary complex formation, it is not technically possible directly to determine  $k_{\text{cat,AMP-Ub}}$ . However, a lower limit can be estimated from the  $k_{\text{cat}}$  for ATP/PP<sub>i</sub> exchange, since the latter assays are measured at equilibrium (17).

models in which the E2 acts as a positive allosteric effector of bound ubiquitin adenylate formation; however, the observation requires that stimulation by HsUbc2b requires Cys<sup>88</sup>. Earlier studies by Pickart *et al.* (44) demonstrated that occupancy of the nucleotide/adenylate site by either ATP·Mg<sup>2+</sup> or ubiquitin adenylate enhanced the rate of E2 transthiolation by ~13-fold. Microscopic reversibility requires that occupancy of the E2 binding site must also stimulate bound ubiquitin adenylate formation. Since HsUbc2bC88A fails to stimulate ubiquitin adenylate formation, the data require that the observed difference between  $k_{\text{cat,AMP-Ub}}$  and  $k_{\text{cat,trans}}$  (Table 2) reflects a positive allosteric effect of bound wild type HsUbc2b on the rate of ubiquitin adenylate formation and that this effect is observed only upon binding of wild type uncharged E2.

The inhibition pattern for the ubiquitin dependence of ATP/PP<sub>i</sub> exchange demonstrates that wild type human Uba1 exhibits pseudo-ordered substrate addition (Fig. 6A) (17). The pseudo-ordered addition mechanism results from the combined effects of differences in binding site geometry and differential relative affinities for ATP·Mg<sup>2+</sup> versus ubiquitin as the leading substrate, requiring that wild type human Uba1 possess a greater affinity for ATP·Mg<sup>2+</sup> as leading substrate than for ubiquitin. Mutation of Asp<sup>576</sup> to either alanine or glutamate shifts GST-HsUba1a to a random addition mechanism, revealed by the hyperbolic ATP/PP<sub>i</sub> exchange kinetics with varying ubiquitin concentration (Fig. 6, B and C). The  $K_m$  values for ATP versus ubiquitin differ too little among the Asp<sup>576</sup> mutants to allow us to propose that the change in binding order results from differential affinities (Table 2). More likely, Asp<sup>576</sup> coordination to Mg<sup>2+</sup> triggers subsequent ubiquitin binding, possibly by opening the channel through which the carboxyl terminus of the latter threads, as revealed from crystal structures for the adenylate binding sites of AppBp1-Uba3 and Sae2-Sae3 (22–24).

The present studies demonstrate that Asp<sup>576</sup> is a critical residue in the catalytic cycle of ubiquitin-activating enzyme for ATP·Mg<sup>2+</sup> binding, substrate binding order, and transition state stabilization that go beyond its originally proposed role based on structural information. However, the complex kinetic phenotype arising from mutation of this group is explained fully by its contributions to substrate and transition state binding. The present data also reveal a previously unrecognized coupling between ATP·Mg<sup>2+</sup> and ubiquitin binding as well as coupling between E2 binding and the rate of ubiquitin adenylate formation.

*Acknowledgments*—We are grateful to Dr. Alan L. Schwartz for kindly providing the pGEX3X-E1 expression plasmid and to Adam Harder for technical support.

## REFERENCES

- Pickart, C. M. (2001) *Annu. Rev. Biochem.* **70**, 503–533
- Hicke, L. (1999) *Trends Cell Biol.* **9**, 107–112
- Jentsch, S., and Pyrowolakis, G. (2000) *Trends Cell Biol.* **10**, 335–342
- Haas, A. L., and Siepmann, T. J. (1997) *FASEB J.* **11**, 1257–1268
- Johnson, E. S., Schwienhorst, R. J., Dohmen, R. J., and Blobel, G. (1997) *EMBO J.* **16**, 5509–5519
- Okuma, T., Honda, R., Ichikawa, G., Tsumagari, N., and Yasuda, H. (1999) *Biochem. Biophys. Res. Commun.* **254**, 693–698
- Liakopoulos, D., Doenges, G., Matuschewski, K., and Jentsch, S. (1998) *EMBO J.* **17**, 2208–2214
- Osaka, F., Kawasaki, H., Aida, N., Saeki, M., Chiba, T., Kawashima, S., Tanaka, K., and Kato, S. (1998) *Genes Dev.* **12**, 2263–2268
- Yuan, W., and Krug, R. M. (2001) *EMBO J.* **20**, 362–371
- Dittmar, G. A., Wilkinson, C. R., Jedrzejewski, P. T., and Finley, D. (2002) *Science* **295**, 2442–2446
- Liu, Y. C., Pan, J., Zhang, C., Fan, W., Collinge, M., Bender, J. R., and Weissman, S. M. (1999) *Proc. Natl. Acad. Sci. U. S. A.* **96**, 4313–4318
- Raasi, S., Schmidtke, G., and Groettrup, M. (2001) *J. Biol. Chem.* **276**, 35334–35343
- Tanida, I., Mizushima, N., Kiyooka, M., Ohsumi, M., Ueno, T., Ohsumi, Y., and Kominami, E. (1999) *Mol. Biol. Cell* **10**, 1367–1379
- Larsen, C. N., and Wang, H. (2002) *J. Proteome Res.* **1**, 411–419
- Schwartz, D. C., and Hochstrasser, M. (2003) *Trends Biochem. Sci.* **28**, 321–328
- Haas, A. L., Warms, J. V., Hershko, A., and Rose, I. A. (1982) *J. Biol. Chem.* **257**, 2543–2548
- Haas, A. L., and Rose, I. A. (1982) *J. Biol. Chem.* **257**, 10329–10337
- Haas, A. L., Warms, J. V., and Rose, I. A. (1983) *Biochemistry* **22**, 4388–4394
- Pickart, C. M., and Rose, I. A. (1985) *J. Biol. Chem.* **260**, 1573–1581
- Leimkuhler, S., Wuebbens, M. M., and Rajagopalan, K. V. (2001) *J. Biol. Chem.* **276**, 34695–34701
- Lake, M. W., Wuebbens, M. M., Rajagopalan, K. V., and Schindelin, H. (2001) *Nature* **414**, 325–329
- Walden, H., Podgorski, M. S., and Schulman, B. A. (2003) *Nature* **422**, 330–334
- Walden, H., Podgorski, M. S., Huang, D. T., Miller, D. W., Howard, R. J., Minor, D. L., Holton, J. M., and Schulman, B. A. (2003) *Mol. Cell* **12**, 1427–1437
- Lois, L. M., and Lima, C. D. (2005) *EMBO J.* **24**, 439–451
- Baboshina, O. V., and Haas, A. L. (1996) *J. Biol. Chem.* **271**, 2823–2831
- Haas, A. L., and Rose, I. A. (1981) *Proc. Natl. Acad. Sci. U. S. A.* **78**, 6845–6848
- Siepmann, T. J., Bohnsack, R. N., Tokgöz, Z., Baboshina, O. V., and Haas, A. L. (2003) *J. Biol. Chem.* **278**, 9448–9457
- Ho, S. N., Hunt, H. D., Horton, R. M., Pullen, J. K., and Pease, L. R. (1989) *Genes (Amst.)* **77**, 51–59
- Bohnsack, R. N., and Haas, A. L. (2003) *J. Biol. Chem.* **278**, 26823–26830
- Segal, I. A. (1975) *Enzyme Kinetics*, Wiley-Interscience, New York
- Burch, T. J., and Haas, A. L. (1994) *Biochemistry* **33**, 7300–7308
- Mitruka, B. M., and Rawnsley, H. M. (1981) *Clinical Biochemical and Hematological Reference Values in Normal Experimental Animals*, Masson Publishers, New York
- Fersht, A. R., Knill-Jones, J. W., Bedouelle, H., and Winter, G. (1988) *Biochemistry* **27**, 1581–1587
- Harmark, K., Anborgh, P. H., Merola, M., Clark, B. F., and Parmeggiani, A. (1992) *Biochemistry* **31**, 7367–7372
- Fan, C., Moews, P. C., Shi, Y., Walsh, C. T., and Knox, J. R. (1995) *Proc. Natl. Acad. Sci. U. S. A.* **92**, 1172–1176
- Ye, D., Wei, M., McGuire, M., Huang, K., Kapadia, G., Herzberg, O., Martin, B. M., and Dunaway-Mariano, D. (2001) *J. Biol. Chem.* **276**, 37630–37639
- Narasimhan, J., Potter, J. L., and Haas, A. L. (1996) *J. Biol. Chem.* **271**, 324–330
- Fersht, A. R. (1987) *Biochemistry* **26**, 8031–8037
- Schmitt, E., Moulinier, L., Fujiwara, S., Imanaka, T., Thierry, J. C., and Moras, D. (1998) *EMBO J.* **17**, 5227–5237
- Desogus, G., Todone, F., Brick, P., and Onesti, S. (2000) *Biochemistry* **39**, 8418–8425
- Fersht, A. R. (1988) *Biochemistry* **27**, 1577–1580
- Wells, T. N., and Fersht, A. R. (1986) *Biochemistry* **25**, 1881–1886
- Borgford, T. J., Gray, T. E., Brand, N. J., and Fersht, A. R. (1987) *Biochemistry* **26**, 7246–7250
- Pickart, C. M., Kasperek, E. M., Beal, R., and Kim, A. (1994) *J. Biol. Chem.* **269**, 7115–7123
- Haas, A. L., Ahrens, P., Bright, P. M., and Ankel, H. (1987) *J. Biol. Chem.* **262**, 11315–11323
- Loeb, K. R., and Haas, A. L. (1992) *J. Biol. Chem.* **267**, 7806–7813